

SCIENTIFIC REPORTS

OPEN

Glaucumolides A and B, Biscembranoids with New Structural Type from a Cultured Soft Coral *Sarcophyton glaucum*

Received: 23 June 2015
Accepted: 29 September 2015
Published: 04 November 2015

Chiung-Yao Huang¹, Ping-Jyun Sung^{2,3}, Chokkalingam Uvarani^{1,2}, Jui-Hsin Su^{2,3}, Mei-Chin Lu^{2,3}, Tsong-Long Hwang⁴, Chang-Feng Dai⁵, Shwu-Li Wu⁶ & Jyh-Horng Sheu^{1,7,8}

Glaucumolides A (1) and B (2), novel biscembranes composed of an unprecedented α,β -unsaturated ϵ -lactone, along with the known metabolites ximaolide A (3) and isosarcophytonolide D (4), were isolated from the cultured soft coral *Sarcophyton glaucum*. The structures of the new metabolites were determined by extensive spectroscopic analyses. Compounds 1 and 2 were shown to exhibit cytotoxicity against a limited panel of cancer cell lines. In anti-inflammation assay, compounds 1 and 2 displayed strong inhibition of superoxide anion generation and elastase release in human neutrophils stimulated by fMLP/CB. Furthermore, both 1 and 2 were shown to significantly inhibit the accumulation of the pro-inflammatory inducible nitric oxide synthase protein, and compounds 1–3 were found to effectively reduce the expression of cyclooxygenase-2 protein, in lipopolysaccharide-stimulated RAW264.7 macrophage cells.

Many cembrane-type diterpenes have been proven to exhibit cytotoxicity and anti-inflammatory activity¹. More than 60 biscembranoids have been isolated from the soft corals of the genera *Sarcophyton*^{2–11}, *Lobophytum*¹², *Sinularia*¹³. In particular, those belonging to the genus *Sarcophyton* are the most prolific source of biscembranoids. A common structural feature among these biscembranes is biogenetically derived from Diels-Alder reaction of two different cembranoid units. In our continuing search for structurally unique bioactive metabolites from the genera *Sarcophyton*¹⁴, we carried out the chemical investigation of the cultured soft coral *Sarcophyton glaucum* (Fig. 1). This study has led to the discovery of two new Diels-Alder cyclized biscembranoids glaucumolides A and B (1 and 2), a known biscembranolide ximaolide A (3)^{8,11}, along with isosarcophytonolide D (4)⁹, an expected biogenic dienophile precursor of 1 (Fig. 2). The structures of 1 and 2 were deduced by extensive spectroscopic analysis. Based on structural consideration, both 1 and 2 were classified as a new type of biscembranoids as they are biosynthesized using ϵ -lactonecebrane 6 as a new diene monomer which has not been discovered before the biosynthesis of biscembranoids formed by Diels-Alder reaction. The attracting biological activities of several known biscembranoids^{13,15} further prompted us to evaluate the cytotoxic and anti-inflammatory activities of isolated metabolites 1–4. The results demonstrated that compounds 1

¹Department of Marine Biotechnology and Resources, National Sun Yat-sen University, Kaohsiung 804, Taiwan.

²National Museum of Marine Biology & Aquarium, Pingtung 944, Taiwan. ³Institute of Marine Biotechnology, National Dong Hwa University, Pingtung 944, Taiwan. ⁴Graduate Institute of Natural Products, School of Traditional Chinese Medicine, College of Medicine, Chang Gung University, Taoyuan 333, Taiwan. ⁵Institute of Oceanography, National Taiwan University, Taipei 112, Taiwan. ⁶General Study Center, National Kaohsiung Marine University, Kaohsiung 805, Taiwan. ⁷Department of Medical Research, China Medical University Hospital, China Medical University, Taichung 404, Taiwan. ⁸Graduate Institute of Natural Products, Kaohsiung Medical University, Kaohsiung 807, Taiwan. Correspondence and requests for materials should be addressed to J.H.S. (email: sheu@mail.nsysu.edu.tw)



Figure 1. The cultured soft coral *Sarcophyton glaucum*.

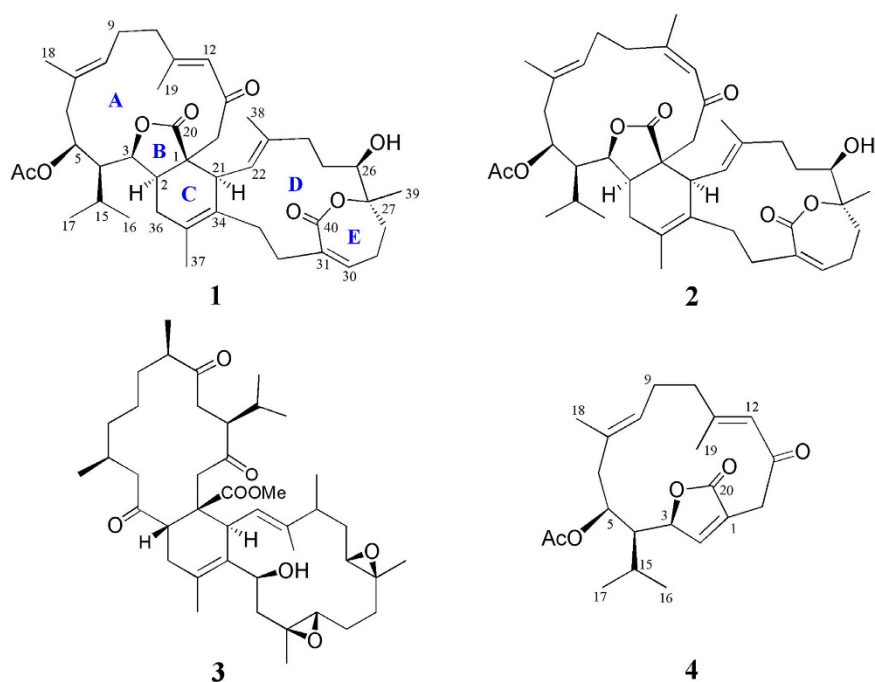


Figure 2. Chemical structures of metabolites 1–4.

and **2**, possessing a γ - and an ϵ -lactone rings, exhibited inhibition against the growth of human cancer cell lines, promyelocytic leukemia (HL-60), leukemic lymphoblasts (CCRF-CEM), acute T lymphoblastic leukaemia (MOLT-4), and erythroleukemia (K-562), as well as anti-inflammatory activities by significantly reducing the superoxide anion generation and elastase release in human neutrophils stimulated by *N*-formyl-methionyl-leucyl-phenylalanine/cytochalasin B (fMLP/CB), and the expression of iNOS and COX-2 proteins in LPS-challenged RAW264.7 macrophage cells. In contrast, without the presence of the mentioned lactone rings, **3** only displayed weaker inhibition on COX-2 accumulation in the same macrophage cells.

Results

Glaucumolide A (**1**), $[\alpha]_D^{25} -207$ (*c* 0.007, CHCl_3), was isolated as an amorphous solid. Its molecular formula, $\text{C}_{42}\text{H}_{58}\text{O}_8$, was established by HRESIMS (713.4022 *m/z*, $[\text{M} + \text{Na}]^+$), implying 14 degrees of unsaturation. The presence of the hydroxyl group was suggested by an absorption band at 3499 cm^{-1} in the IR spectrum. The ^{13}C NMR spectroscopic data of **1** (Table 1) showed the presence of 42 carbon atoms, including eight methyls, 11 methylenes, 11 methines, and 12 quaternary carbons. Its NMR spectrum showed the signals of four vinyl methyls (δ_{H} 2.12, s; 1.81, s; 1.65, s; 1.62, s; δ_{C} 20.2, 19.6, 17.9, 16.0),

Position	1		2	
	¹ H ^a	¹³ C ^b	¹ H ^a	¹³ C ^b
1		53.3 (C)		52.9 (C)
2	2.33 m	41.5 (CH) ^d	1.87 m	41.4 (CH)
3	3.95 dd (11.2, 6.0) ^c	84.4 (CH)	4.01 dd (11.2, 5.6)	85.5 (CH)
4	1.50 d (10.8)	48.7 (CH)	1.85 m	47.3 (CH)
5	4.82 dd (11.2, 3.2)	73.1 (CH)	4.82 dd (11.2, 3.2)	71.9 (CH)
6	2.28 m; 2.24 m	41.0 (CH ₂)	2.26 m; 2.18 m	41.7 (CH ₂)
7		132.5 (C)		131.7 (C)
8	5.14 dd (6.4, 6.4)	127.2 (CH)	5.17 dd (7.6, 7.6)	127.9 (CH)
9	2.32 m	24.7 (CH ₂)	2.29 m; 2.21 m	25.1 (CH ₂)
10	2.31 m; 2.25 m	40.6 (CH ₂)	3.00 m	31.2 (CH ₂)
11		161.1 (C)		162.7 (C)
12	5.78 s	125.0 (CH)	5.98 s	124.6 (CH)
13		197.4 (C)		198.1 (C)
14	2.79 d (13.2); 2.46 d (13.2)	50.7 (CH ₂)	2.99 m; 2.37 m	52.4 (CH ₂)
15	2.20 m	25.7 (CH)	2.17 m	25.6 (CH)
16	1.08 d (6.8)	18.2 (CH ₃)	1.08 d (6.8)	18.4 (CH ₃)
17	1.10 d (6.8)	25.1 (CH ₃)	1.17 d (6.8)	25.0 (CH ₃)
18	1.65 s	17.9 (CH ₃)	1.65 s	17.1 (CH ₃)
19	2.12 s	19.6 (CH ₃)	1.89 s	24.8 (CH ₃)
20		177.9 (C)		179.1 (C)
21	3.05 d (10.0)	45.5 (CH)	2.96 m	45.1 (CH)
22	5.11 d (10.0)	123.0 (CH)	4.94 d (10.8)	122.8 (CH)
23		138.7 (C)		138.3 (C)
24	2.12 m; 2.08 m	36.2 (CH ₂)	2.14 m; 2.02 m	36.4 (CH ₂)
25	1.82 m; 1.36 m	29.1 (CH ₂)	1.84 m; 1.31 m	29.2 (CH ₂)
26	4.16 dd (7.6, 7.6)	68.3 (CH)	4.16 dd (7.6, 7.6)	67.8 (CH)
27		82.9 (C)		82.6 (C)
28	2.18 m; 2.04 m	34.8 (CH ₂)	2.20 m; 2.04 m	34.6 (CH ₂)
29	2.46 m	26.2 (CH ₂)	2.47 m	26.6 (CH ₂)
30	5.93 br s	135.1 (CH)	5.89 br s	135.4 (CH)
31		132.8 (C)		ND ^e
32	2.58 m; 2.18 m	30.0 (CH ₂)	2.65 m; 2.35 m	30.1 (CH ₂)
33	2.66 m; 2.16 m	29.1 (CH ₂)	2.79 m; 2.07 m	29.3 (CH ₂)
34		132.1 (C)		131.3 (C)
35		127.4 (C)		127.4 (C)
36	2.31 m; 2.04 m	34.8 (CH ₂)	2.31 m; 2.10 m	35.3 (CH ₂)
37	1.81 s	20.2 (CH ₃)	1.81 s	20.3 (CH ₃)
38	1.62 s	16.0 (CH ₃)	1.60 s	15.9 (CH ₃)
39	1.32 s	22.0 (CH ₃)	1.31 s	21.8 (CH ₃)
40		168.9 (C)		168.5 (C)
41	2.13 s	21.5 (CH ₃)	2.11 s	21.5 (CH ₃)
42		170.5 (C)		170.6 (C)

Table 1. ¹H and ¹³C NMR Data of **1** and **2**. ^aRecorded at 400 MHz in CDCl₃ at 25 °C. ^bRecorded at 100 MHz in CDCl₃ at 25 °C. ^c*J* values (Hz) in parentheses. ^dAttached protons were deduced by DEPT experiment. ^eDesignate signal not detected¹⁷.

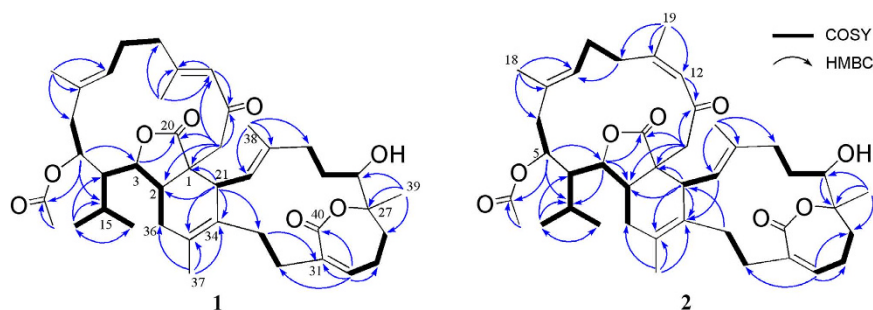


Figure 3. Selected COSY (—) and HMBC (→) correlations of **1** and **2**.

one methyl attached to oxygen-bearing quaternary carbon (δ_{H} 1.32, s; δ_{C} 22.0), one acetoxy group (δ_{H} 2.13, s; δ_{C} 170.5, C; 21.5, CH_3), two methyls of an isopropyl group (δ_{H} 2.20, m; 1.10, d, $J = 6.8$ Hz; 1.08, d, $J = 6.8$ Hz; δ_{C} 25.7, CH; 25.1, CH_3 ; 18.2, CH_3); four trisubstituted double bonds (δ_{H} 5.93, br s; 5.78, s; 5.14, dd, $J = 6.4$, 6.4 Hz; 5.11, d, $J = 10.0$ Hz; δ_{C} 161.1, C; 138.7, C; 135.1, CH; 132.8, C; 132.5, C; 127.2, CH; 125.0, CH; 123.0, CH); one tetrasubstituted double bond (δ_{C} 132.1, C; 127.4, C); three oxygen-bearing methines (δ_{H} 4.82, dd, $J = 11.2$, 3.2 Hz; 4.16, dd, $J = 7.6$, 7.6 Hz; 3.95, dd, $J = 11.2$, 6.0 Hz; δ_{C} 84.4, CH; 73.1, CH; 68.3, CH); one oxygenated quaternary carbon (δ_{C} 82.9), and four carbonyl carbons (δ_{C} 197.4, 177.9, 170.5, 168.9). These evidences indicated the possible presence of a biscembranoid skeleton in compound **1**. The COSY spectrum of **1** was used to identify seven different structural units from H_2 -36 to isopropyl protons H_3 -16 and H_3 -17 via H-2, H-3 and H-4; H-5 to H_2 -6; H-8 to H_2 -10; H-21 to H-22; H_2 -24 to H-26; H_2 -28 to H-30; and H_2 -32 to H_2 -33, which were further assembled by HMBC correlations H-5 to C-3 and C-15; H_2 -14 to C-1, C-2, C-12 and C-13; H_3 -16 and H_3 -17 to C-4 and C-15; H_3 -18 to C-6, C-7 and C-8; H_3 -19 to C-10, C-11 and C-12; H-21 to C-1, C-2, C-33, C-34 and C-35; H-30 to C-31, C-32 and C-40; H_3 -37 to C-34, C-35 and C-36; H_3 -38 to C-22, C-23 and C-24; and H_3 -39 to C-26, C-27 and C-28 (Fig. 3). Moreover, the HMBC correlations of H-3 and H_2 -14 to C-20 clearly suggested the presence of an α,β -unsaturated γ -lactone moiety at C-1–C-3 and C-20. Furthermore, the acetoxy group positioned at C-5 was confirmed from the HMBC correlations of H-5 (δ 4.82, dd, $J = 11.2$, 3.2 Hz) and protons of an acetate methyl (δ 2.13, s) to the ester carbonyl carbon at δ 170.5. In addition, in the ^{13}C NMR spectrum of **1** the signal at δ_{C} 68.3, and in the ^1H NMR spectrum the signal at δ_{H} 4.16 (dd, $J = 7.6$, 7.6 Hz) could be attributed to a hydroxyl-bearing methine at C-26. On the base of above results and by considering the degrees of unsaturation and molecular formula, C-27 and C-40 should be linked by an oxygen atom to form an ϵ -lactone ring. The gross structure of **1** was thus established. Metabolite **1** is the first Diels-Alder cyclized biscembranoid possessing not only a saturated γ -lactone but also a seven-membered α,β -unsaturated ϵ -lactone in the molecule.

The relative configurations of the stereogenic centers in **1** were determined on the basis of NOE relationships and NMR spectroscopic data. It was found that NOESY correlations of H-3 (δ 3.95, dd, $J = 11.2$, 6.0 Hz) with H-2 (δ 2.33, m) and H-5 (δ 4.82, dd, $J = 11.2$, 3.2 Hz), H-4 (δ 1.50, d, $J = 10.8$ Hz) with H-2 and H-5, and H-2 with H-21 (δ 3.05, d, $J = 10.0$ Hz), and the upfield-shifted δ_{H} value of H-21 α relative to the H-21 β of related biscembranoids in ^1H NMR¹⁰, indicated the α -orientation for H-2, H-3, H-4, H-5, and H-21. This observation was also strongly supported by the similar ^1H NMR spectroscopic data of the above protons including chemical shifts and coupling constants with those of bislatumide C¹⁰. Furthermore, the NOE correlations of H-21 with H-33 α (δ 2.16, m) and H_3 -38, H_3 -38 with H-26 (δ 4.16, dd, $J = 7.6$, 7.6 Hz), and H-26 with H-25 α (δ 1.82, m), H-29 α (δ 2.46, m) and H-30 (δ 5.93, br s), reflected the α -orientations of H-26 and the R^* -configuration at C-26. Above results and the NOE correlation between H_3 -39 (δ 1.32, s) and H-25 β (δ 1.36, m) suggested the β -orientation of H_3 -39 and thus 27 S^* configuration of **1** as shown in Fig. 4. Further, the 26 R^* and 27 S^* configuration, not 26 R^* and 27 R^* , could be confirmed by comparing the δ values of C-7 (69.2) and C-8 (82.9) of known compound sartrolide C¹⁶ to the corresponding C-26 (68.3) and C-27 (82.9) of **1**, while sartrolide A¹⁶ with 26 R^* and 27 R^* configuration showed C-26 signal at δ 72.7 ppm. The chemical shift values of C-18 (17.9), C-19 (19.6) and C-38 (16.0) reflected the all *trans* geometry of the trisubstituted double bonds at C-7/C-8, C-11/C-12 and C-22/C-23 in the molecule of **1**. From the above observations, NOE correlation between H-30 and one of H_2 -33 (δ 2.66, m), and further analysis of other NOE interactions (Fig. 4), the relative configuration of **1** with rings A–E could be established.

Glaucumolide B (**2**), $[\alpha]_{\text{D}}^{25} -221$ (c 0.008, CHCl_3), was showed the pseudomolecular ion peak $[\text{M} + \text{Na}]^+$ at m/z 713.4023 in the HRESIMS, suggesting the molecular formula $\text{C}_{42}\text{H}_{58}\text{O}_8$ and 14 degrees of unsaturation. The IR spectrum also suggested the presence of hydroxyl group in **2** (ν_{max} 3434 cm^{-1}). The ^{13}C NMR spectroscopic data (Table 1) of **2** were found to be resembled to those of **1**. Detailed analysis of 1D and 2D NMR spectra of **2** revealed the similar gross structure as that of **1**. However, it was found that H-12 (δ 5.98, s) showed significant NOE interaction with H_3 -19 (δ 1.89, s), and the signal of the C-19 in **2** was remarkably downfield-shifted (δ 19.6 in **1**, 24.8 in **2**), indicating a *Z* geometry of

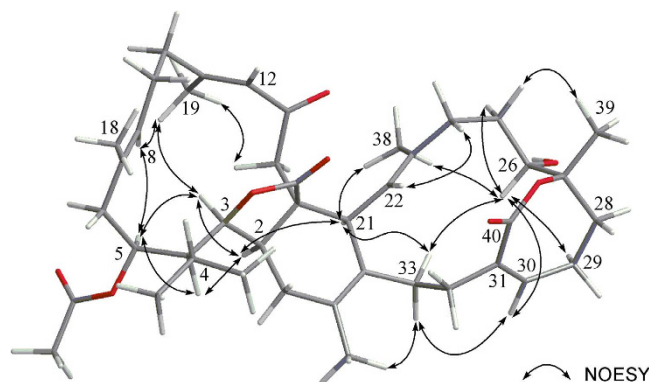


Figure 4. Selected NOE correlations for 1.

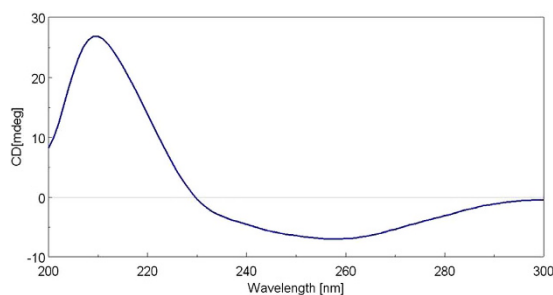


Figure 5. CD spectrum (1.2×10^{-4} M, MeOH) of 2.

$\Delta^{11(12)}$ in **2**, in contrast to the 11*E* double bond in **1**. These results and other NMR data including NOE correlations, established the structure of compound **2** to be the 11*Z* isomer of **1**.

The absolute configurations of **1** and **2** were further confirmed by comparison of the CD (circular dichroism) spectroscopic data with structurally related compound. As shown in Fig. 5, the CD spectrum of **2** showed a broad negative Cotton effect at 258 nm ($\Delta\epsilon = -7.1$) due to enone $n \rightarrow \pi^*$ transition absorption while the intense positive cotton effect at 209 nm ($\Delta\epsilon = +27.4$) resulted from the $\pi \rightarrow \pi^*$ transition of the two isolated $\Delta^{22(23)}$ and $\Delta^{34(35)}$ double bonds, very similar to that of bislatumlide **C**¹⁰. Thus, the absolute configurations for rings B and C should be the same for both bislatumlide **C** and **2**. One the basis of above results and the fact that both **1** and **2** were isolated from the same organism, the structures and absolute configurations of both **1** and **2** were found to possess the 1*S*,2*R*,3*S*,4*S*,5*S*,21*S*,26*R*,27*S*.

A plausible biosynthetic pathway, involving a key Diels–Alder reaction, was postulated for the biosynthesis of compounds **1** and **2** in Figure 6. It is obvious that **4** is one of the two precursors of **1**. Another proposed precursor should be the yet to be discovered compound **6**. [4+2] Endo cycloaddition of the dienophile **4** and diene **6** occurs between 1,2-Z double bond of **4** and $\Delta^{21(34)}$ and $\Delta^{35(36)}$ conjugated double bonds diene of **6**. Although the possible involvement of a biosynthetic Diels–Alder reaction to afford biscembranoid has been mentioned frequently, no any other biscembranoid was found to be formed by using ϵ -lactone cembrane **6** or related cembranoidal ϵ -lactone as the diene precursor. In addition, almost all the previous cembrane dimers exhibited the reactive dienophile double bond at positions C-1 and C-14 (according to the numbering assigned to compound **4**), whereas the dienophile double bond in **4** was located at C-1 and C-2. The Diels–Alder addition which arises from supra–supra transition state explains the *trans* stereochemistry of H-2 and lactone as well as the *cis* geometry of lactone and H-21. Analogously, the formation of biscembrane **2** by Diels–Alder cyclization of the 11Z isomer of **4**, sarcophytonolide A (**5**)^{6,9}, with compound **6** could be hypothesized.

The cytotoxicity of compounds **1**–**4** against four human cancer cell lines, HL-60, CCRF-CEM, MOLT-4, and K-562 was investigated. The results (Table 2) demonstrated that compound **2** exhibited significant cytotoxicity against HL-60 and CCRF-CEM cancer cell lines with ED₅₀ values of 3.8 ± 0.9 and 5.3 ± 1.4 µg/mL, respectively. Also, compound **1** exhibited cytotoxicity against the above two cell lines with ED₅₀ values of 6.6 ± 1.2 and 7.4 ± 1.5 µg/mL, respectively. Further, compounds **1** and **2** displayed weaker activity against MOLT-4 and K-562 cell lines (ED₅₀ 11.0–19.2 µg/mL). In contrast, compound **3** was inactive toward all the tested cell lines. Perhaps the enhanced cytotoxicity of compounds **1** and **2** relative to **3** is owing to the presence of a α,β-unsaturated ε-lactone ring.

The anti-inflammatory activities of compounds **1-4** on neutrophil pro-inflammatory responses were evaluated by measuring their ability in suppressing fMLP/CB-induced superoxide anion ($O_2^{\cdot -}$)

cancer cell line	Compounds (ED ₅₀ , $\mu\text{g/mL}$)				
	1	2	3	4	5-Fluorouracil
HL-60	6.6 \pm 1.2	3.8 \pm 0.9	— ^a	13.0 \pm 1.9	10.7 \pm 0.5
CCRF-CEM	7.4 \pm 1.5	5.3 \pm 1.4	—	15.3 \pm 2.5	2.3 \pm 0.6
MOLT-4	11.0 \pm 2.8	11.0 \pm 2.2	—	17.2 \pm 3.1	0.9 \pm 0.2
K-562	19.2 \pm 2.3	12.6 \pm 0.7	—	—	4.3 \pm 1.2

Table 2. Cytotoxicity of compounds 1–4. The values are mean \pm SEM ($n = 3$). ^a— $>20 \mu\text{g/mL}$

Compound	Superoxide anion			Elastase release		
	IC ₅₀ (μM) ^b	Inh % ^a		IC ₅₀ (μM)	Inh %	
1	2.79 \pm 0.66	88.42 \pm 3.97	***	3.97 \pm 0.10	88.94 \pm 6.96	***
2	2.79 \pm 0.32	91.75 \pm 3.08	***	3.97 \pm 0.10	103.25 \pm 1.89	***
3	>10	15.33 \pm 4.15	*	>10	15.13 \pm 3.58	*
4	>10	12.40 \pm 2.56	**	>10	27.12 \pm 3.08	***
Idelalisib	0.07 \pm 0.01	102.81 \pm 2.21	***	0.28 \pm 0.09	99.56 \pm 4.19	***

Table 3. Inhibitory effects of compounds 1–4 on superoxide anion generation and elastase release by human neutrophils. ^aPercentage of inhibition (Inh %) at $10 \mu\text{M}$ concentration. Results are presented as mean \pm S.E.M. ($n = 3$). * $P < 0.05$, ** $P < 0.01$, *** $P < 0.001$ compared with the control value. ^bConcentration necessary for 50% inhibition (IC₅₀).

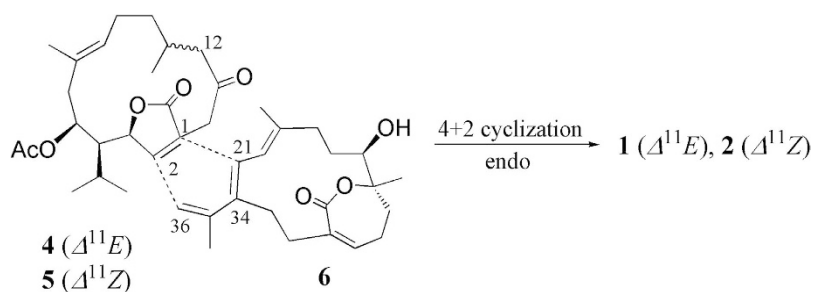


Figure 6. Plausible Diels-Alder reaction to derive compounds 1 and 2.

generation and elastase release in human neutrophils, and the results were shown in Table 3. From the results, 1 and 2 showed strong inhibitions (88.42 ± 3.97 and $91.75 \pm 3.08\%$, respectively.) toward superoxide anion generation at $10 \mu\text{M}$. Both of them also exhibited potent inhibitory activity against elastase release, with 88.94 ± 6.96 and $103.25 \pm 1.89\%$ inhibitions in the same fMLP/CB-stimulated cells at the same concentration. The IC₅₀ values of 1 and 2 in inhibiting the superoxide generation and elastase release were also measured. Although compound 4 did not exhibit strong activity in inhibiting superoxide anion generation, it was shown to display significant inhibitory activity in elastase release.

The *in vitro* anti-inflammatory activity of compounds 1–3 was also studied. In this assay, the up-regulation of the proinflammatory iNOS and COX-2 proteins of LPS-stimulated RAW264.7 macrophage cells was evaluated using immunoblot analysis. The results (Fig. 7) showed that at concentrations of 5, 10, and $20 \mu\text{M}$, compound 1 was found to significantly reduce the levels of iNOS and COX-2 to 59.4 ± 9.0 and $66.5 \pm 4.4\%$; 31.3 ± 6.5 and $78.3 \pm 5.0\%$; and -2.6 ± 2.7 and $-0.5 \pm 3.2\%$, respectively. At concentrations of 10 and $20 \mu\text{M}$, compound 2 was found to significantly reduce the levels of iNOS and COX-2 to 75.9 ± 3.5 and $64.3 \pm 6.9\%$; and 43.4 ± 5.0 and $6.0 \pm 3.6\%$, respectively. Moreover, at $20 \mu\text{M}$, 3 also reduced the level of COX-2 expression to $22.0 \pm 6.5\%$ in macrophage cells with LPS treatment. As they did not exhibit cytotoxicity to RAW264.7 cells, they might be promising anti-inflammatory agents. Also, 2 possessing promising cytotoxicity, could become a candidate for future anticancer drug development.

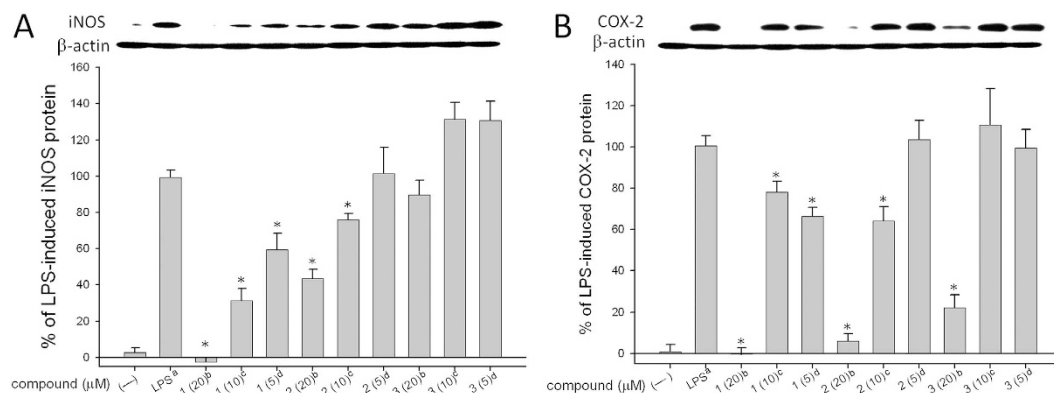


Figure 7. Effect of compounds 1–3 on iNOS and COX-2 protein expression of RAW264.7 macrophage cells by immunoblot analysis. (A) Immunoblots of iNOS and β -actin; (B) Immunoblots of COX-2 and β -actin. The values are mean \pm SEM ($n = 3$). Relative intensity of the LPS alone stimulated group was taken as 100%. Under the same experimental condition CAPE (caffeic acid phenylethyl ester, 10 μ M) reduced the levels of the iNOS and COX-2 to $2.5 \pm 3.7\%$ and $50.3 \pm 8.7\%$, respectively. *Significantly different from LPS alone stimulated group ($p < 0.05$). ^aStimulated with LPS. ^bStimulated with LPS in the presence of 1–3 (20 μ M). ^cStimulated with LPS in the presence of 1–3 (10 μ M). ^dStimulate with LPS in the presence of 1–3 (5 μ M).

Discussion

Compounds **1** and **2** are structurally novel as they belong to a new type of biscembranoids using the not yet isolated ϵ -lactonecembrane **6** as the first time discovered diene precursor for the biosynthesis of biscembranoids by Diels-Alder reaction. Metabolites **1** and **2**, with the presence of a α,β -unsaturated ϵ -lactone ring, were shown to exhibit cytotoxicity against a limited panel of HL-60, CCRF-CEM, MOLT-4 and K-562 cancer cell lines. Compounds **1** and **2** also exhibited potent anti-inflammatory activity in inhibiting the superoxide generation and elastase release in fMLP/CB-induced human neutrophils. Furthermore, both **1** and **2** were shown to significantly inhibit the accumulation of the pro-inflammatory inducible nitric oxide synthase protein, and compounds **1–3** were found to effectively reduce the expression of cyclooxygenase-2 protein, in lipopolysaccharide-stimulated RAW264.7 macrophage cells.

Conclusion

The unusual structural framework with α,β -unsaturated ϵ -lactone system were reported here for glaucumolides A and B (**1** and **2**), along with a known biscembranolide ximaolide A (**3**), and isosarcophytonolide D (**4**) from the cultured soft coral *S. glaucum*. From the results of biological activities, it appears that compounds **1** and **2** might be useful for future biomedical applications. The discovery of glaucumolides with a novel carbon scaffold provides additional evidence that cultured soft corals might be a promising source of structurally novel bioactive natural products which could be used for further pharmacological investigation.

Methods

General Experimental Procedures. Optical rotations were measured on a Horiba High Sensitivity Polarimeter SEPA-300. Ultraviolet spectra were recorded on a JASCO V-650 spectrophotometer. IR spectra were recorded on a JASCO FT/IR-4100 infrared spectrophotometer. CD spectra were recorded on a JASCO J-815 CD spectrophotometer. NMR spectra were recorded on a Varian 400MR FT-NMR instrument at 400 MHz for ^1H and 100 MHz for ^{13}C in CDCl_3 . LRMS and HRMS were obtained by ESI on a Bruker APEX II mass spectrometer. Silica gel (Merck, 230–400 mesh) was used for column chromatography. Precoated silica gel plates (Merck, Kieselgel 60 F-254, 0.2 mm) were used for analytical TLC. High-performance liquid chromatography was performed on a Hitachi L-2455 HPLC apparatus with a Supelco C18 column (250 \times 21.2 mm, 5 μ m).

Animal Material. The cultured soft coral *Sarcophyton glaucum* used in this study was originally collected from the wild and cultured for five years in an 80-ton cultivation tank (height 1.6 m) located in the National Museum of Marine Biology and Aquarium, Taiwan. The tank was a semiclosed recirculating aquaculture system and did not require deliberate feeding. To the best of our knowledge, this is the first farming system for *S. glaucum* in the world. The specimens were then collected by hand in January 2010 and were stored in a -20°C freezer. The soft coral was identified by one of the authors (C.-F.D.). A voucher specimen (specimen no. 201001C3) was deposited in the Department of Marine Biotechnology and Resources, National Sun Yat-sen University.

Extraction and Isolation. The frozen bodies of *S. glaucum* (0.6 kg, wet wt) were minced and extracted exhaustively with CH_2Cl_2 and MeOH (1:1, 0.5 L \times 6). The CH_2Cl_2 and MeOH extract of the soft coral *S. glaucum* was partitioned between EtOAc and H_2O to afford the EtOAc-soluble fraction. The EtOAc extract (4.5 g) was chromatographed over silica gel by column chromatography and eluted with EtOAc in *n*-hexane (0–100%, stepwise) and then with MeOH in EtOAc (5–50%, stepwise) to yield 24 fractions. Fraction 15 (23.3 mg), eluting with *n*-hexane–EtOAc (5:1), was further purified by reversed-phase HPLC using MeOH– H_2O (3:1) to afford **4** (2.6 mg). Fraction 20 (69.7 mg), eluting with *n*-hexane–EtOAc (1:1), was further purified over silica gel using *n*-hexane–acetone (2:1) to afford six subfractions (A1–A6). Subfraction A3 (13.5 mg) was further purified by reversed-phase HPLC using MeOH– H_2O (5:2) to afford **3** (5.2 mg). Subfraction A4 (20.0 mg) was further purified by reversed-phase HPLC using MeOH– H_2O (2:1) to afford **1** (4.4 mg) and **2** (2.8 mg).

Glaucumolide A (1). white amorphous powder; $[\alpha]_D^{25} -207$ (c 0.007, CHCl_3); IR (neat) ν_{max} 3499, 2939, 2876, 1734, 1716, 1699, 1375, 1239, 1024, and 755 cm^{-1} ; UV (MeOH) λ_{max} (log ϵ) 205 (3.4) and 236 (3.2) nm; CD (1.9×10^{-4} M, MeOH) λ_{max} ($\Delta\epsilon$) 244 (–23.7), and 215 (+36.0) nm; ^{13}C and ^1H NMR data, see Table 1; ESIMS m/z 713 $[\text{M} + \text{Na}]^+$; HRESIMS m/z 713.4022 $[\text{M} + \text{Na}]^+$ (calcd for $\text{C}_{42}\text{H}_{58}\text{O}_8\text{Na}$, 713.4024).

Glaucumolide B (2). white amorphous powder; $[\alpha]_D^{25} -221$ (c 0.008, CHCl_3); IR (neat) ν_{max} 3434, 2940, 2878, 1734, 1716, 1698, 1376, 1239, 1024, and 754 cm^{-1} ; UV (MeOH) λ_{max} (log ϵ) 205 (3.3) and 236 (3.2) nm; CD (1.2×10^{-4} M, MeOH) λ_{max} ($\Delta\epsilon$) 258 (–7.1), and 209 (+27.4) nm; ^{13}C and ^1H NMR data, see Table 1; ESIMS m/z 713 $[\text{M} + \text{Na}]^+$; HRESIMS m/z 713.4022 $[\text{M} + \text{Na}]^+$ (calcd for $\text{C}_{42}\text{H}_{58}\text{O}_8\text{Na}$, 713.4023).

Cytotoxicity Testing. Cell lines were purchased from the American Type Culture Collection (ATCC). Cytotoxicity assays of compounds **1–4** were performed using the Alamar Blue assay^{18,19}. To measure the cytotoxicity activities of tested compounds, three concentrations in DMSO with three replications were performed on each cell line. 5-Fluorouracil and DMSO were used as positive and negative controls, respectively in this assay.

Preparation of Human Neutrophils. Human neutrophils obtained from peripheral blood of healthy adult volunteers (20–30 years old) were enriched using a standard method of dextran sedimentation, Ficoll-Hypaque centrifugation, and hypotonic lysis^{20,21}. Purified neutrophils were resuspended in a Ca^{2+} -free HBSS buffer (pH 7.4) at 4 °C prior to use.

Measurement of $\text{O}_2^{\cdot -}$ Generation. The $\text{O}_2^{\cdot -}$ production was assayed based on the superoxide oxide dismutase inhibitable reduction of ferricytochrome *c*^{22–24}. Briefly, neutrophils (6×10^5 cells/mL) incubated with ferricytochrome *c* (0.5 mg/mL) and Ca^{2+} (1 mM) were equilibrated at 37 °C for 2 min and then treated with DMSO as control or different concentrations of compounds for 5 min. Neutrophils were activated by 100 nM fMLP for 10 min in the pretreatment of cytochalasin B (CB, 1 $\mu\text{g}/\text{mL}$) for 3 min (fMLP/CB).

Measurement of Elastase Release. The elastase release was assayed using MeO-Suc-Ala-Ala-Pro-Val-*p*-nitroanilide as the enzyme substrate^{23,24}. Briefly, neutrophils (6×10^5 cells/mL) incubated with MeO-Suc-Ala-Ala-Pro-Val-*p*-nitroanilide (100 μM) were equilibrated at 37 °C for 2 min and treated with compounds for 5 min. Neutrophils were then activated with fMLP (100 nM)/CB (0.5 $\mu\text{g}/\text{mL}$) for 10 min.

Statistical Analysis. Results are expressed as the mean \pm SEM, and comparisons were made using Student's *t*-test. A probability value of 0.05 or less was considered significant. The software SigmaPlot was used for the statistical analysis.

In Vitro Anti-Inflammatory Assay. Macrophage (RAW264.7) cells were purchased from ATCC. *In vitro* anti-inflammatory activities of compounds **1–3** were measured by examining the inhibition of lipopolysaccharide (LPS) induced upregulation of iNOS (inducible nitric oxide synthetase) and COX-2 (cyclooxygenase-2) proteins in macrophages cells using Western blotting analysis²⁵. For statistical analysis, all of the data were analyzed by a one-way analysis of variance (ANOVA), followed by the Student-Newman-Keuls *post hoc* test for multiple comparisons. A significant difference was defined as a *p* value of <0.05 .

References

- Blunt, J. W. *et al.* Marine natural products. *Nat. Prod. Rep.* **32**, 116–211 (2015).
- Su, J. Y., Long, K. H. & Peng, T. S. The structure of methyl isosartortuoate, a novel tetracyclic tetraterpenoid from the soft coral *Sarcophyton tortuosum*. *J. Am. Chem. Soc.* **108**, 177–178 (1986).

3. Kusumi, T. *et al.* J. A novel chlorinated biscembranoid from the marine soft coral *Sarcophyton glaucum*. *J. Org. Chem.* **55**, 6286–6289 (1990).
4. Leone, P. A., Carroll, A. R., Coll, J. C. & Meehan, G. V. Studies of Australian soft corals, XLIX. A new biscembranoid and its probable biosynthetic precursors from the soft coral *Sarcophyton tortuosum*. *J. Nat. Prod.* **56**, 521–526 (1993).
5. Feller, M. *et al.* Isoprenoids of the soft coral *Sarcophyton glaucum*: Nyalolide, a new biscembranoid, and other terpenoids. *J. Nat. Prod.* **67**, 1303–1308 (2004).
6. Jia, R., Guo, Y. W., Mollo, E. & Cimino, G. Sarcophytonolides A–D, four new cembranolides from the Hainan soft coral *Sarcophyton* sp. *Helv. Chim. Acta* **88**, 1028–1033 (2005).
7. Iwagawa, T. *et al.* Biscembranes from the soft coral *Sarcophyton glaucum*. *J. Nat. Prod.* **69**, 1130–1133 (2006).
8. Jia, R. *et al.* Biscembranoids and their probable biogenetic precursor from the Hainan Soft Coral *Sarcophyton tortuosum*. *J. Nat. Prod.* **70**, 1158–1166 (2007).
9. Yan, X. H., Gavagnin, M., Cimino, G. & Guo, Y. W. Two new biscembranes with unprecedented carbon skeleton and their probable biogenetic precursor from the Hainan soft coral *Sarcophyton latum*. *Tetrahedron Lett.* **48**, 5313–5316 (2007).
10. Jia, R. *et al.* Biscembranoids formed from an α,β -unsaturated γ -lactone ring as a dienophile: structure revision and establishment of their absolute configurations using theoretical calculations of electronic circular dichroism spectra. *J. Org. Chem.* **78**, 3113–3119 (2013).
11. Li, Y. F. *et al.* Structural revision of methyl tortuosate D, a bis-cembranoid from Hainan *Sarcophyton tortuosum* and its absolute stereochemistry. *J. Asian Nat. Prod. Res.* **15**, 566–573 (2013).
12. Yan, P., Lv, Y., Ofwegen, L. V., Proksch, P. & Lin, W. Lobophytones A–G, new isobiscembranoids from the soft coral *Lobophytum pauciflorum*. *Org. Lett.* **12**, 2484–2487 (2010).
13. Chen, B. W. *et al.* A novel symmetric sulfur-containing biscembranoid from the Formosan soft coral *Simularia flexibilis*. *Tetrahedron Lett.* **51**, 5764–5766 (2010).
14. Lin, K. H. *et al.* Tortuosenes A and B, new diterpenoid metabolites from the Formosan soft coral *Sarcophyton tortuosum*. *Org. Lett.* **16**, 1314–1317 (2014).
15. Nhiem, N. X. *et al.* Biscembranoids from the marine sponge *Petrosia nigricans*. *Nat. Prod. Commun.* **8**, 1209–1212 (2013).
16. Liang, L. F., Lan, L. F., Tagliatella-Scafati, O. & Guo, Y. W. Sartrolides A–G and bissartrolide, new cembranolides from the South China Sea soft coral *Sarcophyton trocheliophorum* Marenzeller. *Tetrahedron* **69**, 7381–7386 (2013).
17. Iwagawa, T. *et al.* Cytotoxic biscembranes from the soft coral *Sarcophyton glaucum*. *J. Nat. Prod.* **72**, 946–949 (2009).
18. Nakayama, G. R., Caton, M. C., Nova, M. P. & Parondoosh, Z. J. Assessment of the Alamar Blue assay for cellular growth and viability *in vitro*. *Immunol. Methods* **204**, 205–208 (1997).
19. O'Brien, J., Wilson, I., Orton, T. & Pognan, F. I. Investigation of the Alamar Blue (resazurin) fluorescent dye for the assessment of mammalian cell cytotoxicity. *Eur. J. Biochem.* **267**, 5421–5426 (2000).
20. Boyum, A. & Scand, J. Isolation of mononuclear cells and granulocytes from human blood. Isolation of mononuclear cells by one centrifugation, and of granulocytes by combining centrifugation and sedimentation at 1 g. *Clin. Lab. Invest.* **97**, 77–89 (1968).
21. Jauregui, H. O. *et al.* Trypan blue dye uptake and lactate dehydrogenase in adult rat hepatocytes-freshly isolated cells, cell suspensions, and primary monolayer cultures. *In Vitro* **17**, 1100–1110 (1981).
22. Babior, B. M., Kipnes, R. S. & Curnutte, J. T. Biological defense mechanisms. The production by leukocytes of superoxide, a potential bactericidal agent. *J. Clin. Invest.* **52**, 741–744 (1973).
23. Hwang, T. L., Leu, Y. L., Kao, S. H., Tang, M. C. & Chang, H. L. Viscolin, a new chalcone from *Viscum coloratum*, inhibits human neutrophil superoxide anion and elastase release via a cAMP-dependent pathway. *Free Radical Biol. Med.* **41**, 1433–1441 (2006).
24. Yang, S. C. *et al.* Propofol inhibits superoxide production, elastase release, and chemotaxis in formyl peptide-activated human neutrophils by blocking formyl peptide receptor 1. *J. Immunol.* **190**, 6511–6519 (2013).
25. Wen, Z. H., Chao, C. H., Wu, M. H. & Sheu, J. H. A neuroprotective sulfone of marine origin and the *in vivo* anti-inflammatory activity of an analogue. *Eur. J. Med. Chem.* **45**, 5998–6004 (2010).

Acknowledgements

This work was supported by grants from the the National Science Council (NSC-100-2320-B-110-001-M2 and NSC 102-2628-B-110-002-MY2), and Ministry of Education (01C030205) of Taiwan awarded to J.-H.S.

Author Contributions

J.-H.S. designed the whole experiment and contributed to manuscript preparation. C.-Y.H., P.-J.S. and C.U. carried out the experiment and wrote the manuscript. C.-Y.H., J.-H.S. and S.-L.W. performed the isolation of compounds and the analysis of NMR and MS data. C.-Y.H., M.-C.L. and T.-L.H. performed and analyzed the bioassay. C.-F.D. identified the soft coral. All authors reviewed the manuscript.

Additional Information

Competing financial interests: The authors declare no competing financial interests.

How to cite this article: Huang, C.-Y. *et al.* Glaucumolides A and B, Biscembranoids with New Structural Type from a Cultured Soft Coral *Sarcophyton glaucum*. *Sci. Rep.* **5**, 15624; doi: 10.1038/srep15624 (2015).



This work is licensed under a Creative Commons Attribution 4.0 International License. The images or other third party material in this article are included in the article's Creative Commons license, unless indicated otherwise in the credit line; if the material is not included under the Creative Commons license, users will need to obtain permission from the license holder to reproduce the material. To view a copy of this license, visit <http://creativecommons.org/licenses/by/4.0/>